THE KERAMIK THERMAL PROTECTION SYSTEM EXPERIMENT ON THE FOTON-M2 MISSION

T. Reimer[(1)]

[(1)] *DLR, Institute of Structures and Design, Stuttgart, Germany*

ABSTRACT

On June 16, 2005 the re-entry module of the Russian FOTON-M2 spacecraft made a successful landing after a 16-day microgravity mission in space. On board was also the "KERAMIK" experiment by the Institute of Structures and Design of the German Aerospace Center (DLR) in Stuttgart, Germany. The re-entry technology experiment was aiming for the first flight of a Thermal Protection System (TPS) with it´s structural components designed and manufactured fully in C/C-SiC, a Ceramic Matrix Composite (CMC) material developed by DLR.

The experiment had a surface diameter of 340 mm and was located on the exterior of the re-entry spacecraft embedded into the ablative heat shield. The emphasis of the experiment was on the system aspects of the TPS design. It included two stiffened surface panels each fixed to three structural posts with a special fastener type, all components made from the C/C-SiC material. The experiment deliberately included a gap between the panels and a surrounding close-out ring to test the performance of a dedicated seal in that area. In addition to the structural aspects of the experiment, a set of different oxidation protection coatings was applied to the surface of one of the panels to conduct a comparative test under flight conditions.

The position of the experiment was carefully selected with regard to the aerothermodynamic environment. Since the experiment technology aims at re-usable vehicles, a position in the stagnation area of the ballistic re-entry module would have resulted in excessive heat loads. Therefore a location was preferred at an angle of almost 90° relative to the flight direction. The temperature data that was measured during re-entry shows that the surface temperature was close to 1500°C, which was in the targeted range. The structural components on the surface of the experiment were in an excellent condition as a visual inspection immediately after landing revealed.

1. INTRODUCTION

A candidate material for the use in new TPS designs for reusable space vehicles are Ceramic Matrix Composites. DLR has been working this issue and has developed it´s own material type, referred to as C/C-SiC. It is based on carbon fibres embedded in a silicon carbide matrix and is produced via melt infiltration of liquid silicon into a porous C/C component [1].

In recent years, DLR has contributed to TPS developments in many ways. Material samples and structures were flown on re-entry vehicles in flight experiments in earlier FOTON and in the EXPRESS missions [2]. TPS design solutions and components were developed and tested in ground facilities in the ESA-FESTIP programme [3]. Standing out from these developments, the complete nose cap for the NASA X-38 vehicle was manufactured and installed on the flight vehicle, which never made it into space [4].

2. EXPERIMENT OBJECTIVES

The experiment goal was to verify the system concept for a rigid-surface CMC TPS in a full re-entry. The main objectives were to verify whether the surface components are damaged after flight, especially at their edges and corners with regard to the inherent gaps in the system design. Then the question of sufficient sealing was to be answered and the performance of the fastening and attachment concept was of big interest. In addition, the flight provided for the opportunity to collect rare flight data with regard to the re-entry environment.

3. EXPERIMENT DESIGN

The experiment design includes all components that are considered essential for a future TPS on a reusable vehicle. Especially the attachment and fastening components are also made from CMC to make full use of the material capabilities in a high temperature environment. Since a rigid surface TPS is confronted with the sealing problem between adjacent surface panels, the design includes a separation gap between two panels to verify the interface and the underlying seal. In addition, different oxidation protection coatings were applied on one of the panels for comparative testing.

The experiment design is based on developments that reach back to the ESA-FESTIP programme. However, the design includes a number of advancements. The main design features are:

- Two stiffened C/C-SiC panels enclosed by a C/C-SiC interface ring
- Load introduction via three C/C-SiC components per panel
- One stiff and two flexible posts per panel.
- C/C-SiC fasteners for the panel attachment.
- Seal underneath the gaps between the panel edges.
- Spherical panel surfaces.
- Experiment thickness of 23,5mm including the aluminum carrier plate.

The diameter of the C/C-SiC interface ring is 340mm, the diameter of the panels is 300mm. The panels are spherical with L-profile stiffeners and are manufactured using the in-situ joining technology.

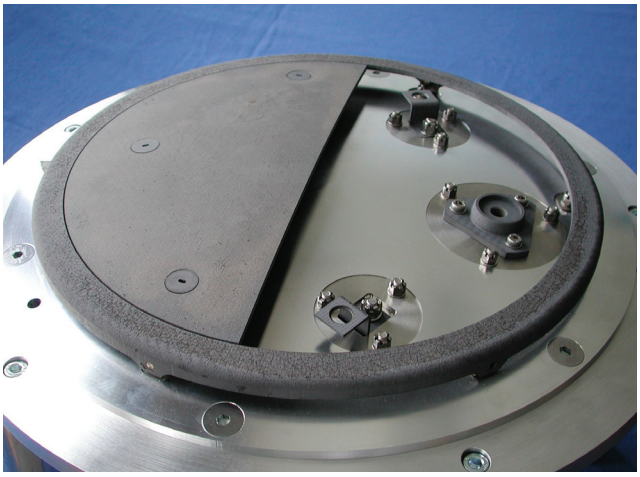

Figure 1: Structural concept of the experiment.

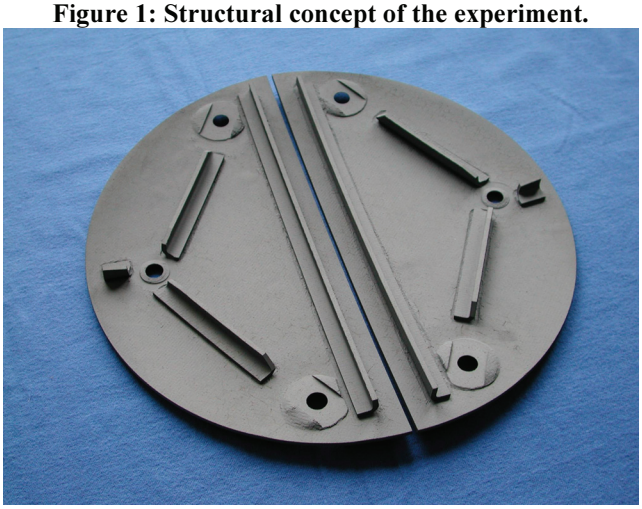

Figure 2: Surface panel internal view.

All the posts are made from C/C-SiC, as well as the fasteners and nuts. Due to this straightforward design, the temperature potential of the material can be used to the full extent, with no limitations by the use of metallic components. The post design and their locations provide for thermal expansion mismatch compensation between panels and substructure. One of the posts serves as the center point with regard to thermal expansion and is designed as a stiff conical tube, called the central post. The others are shaped as z-posts and are located in the far corners of the surface panels.

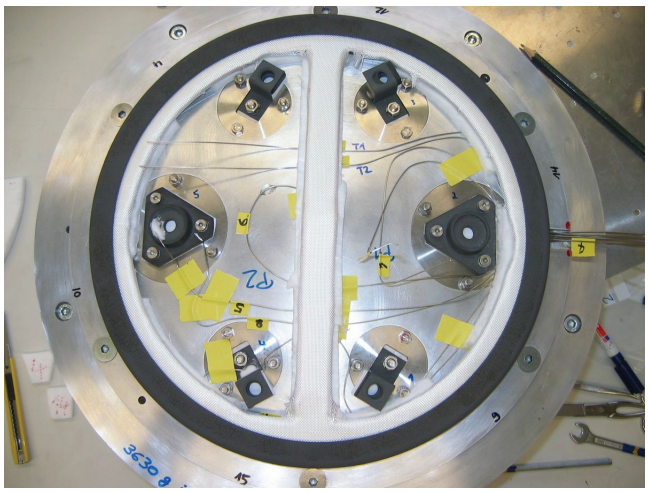

Figure 3: Attachment posts, interface ring and seal.

The experiment was designed to incorporate gaps and a seal to close them. Two semi-circle panels of 300 mm diameter are surrounded by an interface ring which is bonded into the ablator. A seal was placed below the gap between the panels and between the panels and the interface ring to prevent hot gas from entering. That seal was designed relying on the experience gathered from the X-38 developments. It includes basically a thin C/C-SiC structure, covered with a layer of ceramic felt and is altogether wrapped in a ceramic cloth.

A set of three different oxidation protection coatings was applied on the downstream panel on top of the standard coating to conduct a comparative test.

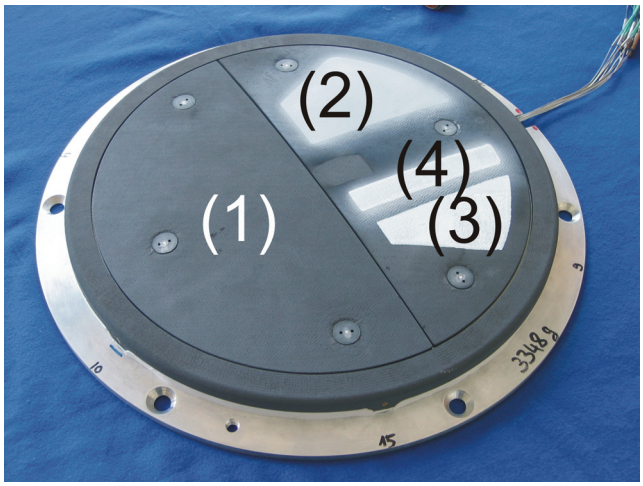

Figure 4: Oxidation protection coatings.

A layer of CVD-SiC (1) is applied to all surfaces as the standard protection. On top of this layer, two other

coatings are applied in combinations. Yttrium-silicate (2) as well as titanium-dioxide (3) were chosen as promising candidates. Finally, a combination of these, with Yttrium-silicate below and titanium-dioxide on top was applied (4).

A number of 9 thermocouples were integrated, as well as one accelerometer that was placed in the capsule internal. A CIMT (crystal indicators of maximum temperatures) peak temperature measurement developed in Russia was also applied. It is based on the alteration of physical properties in crystals subjected to a temperature load. After flight the peak temperature can be determined.

The experiment location on the capsule was chosen with regard to the aerothermodynamic environment relevant for a reusable vehicle. As the stagnation point temperature and pressure are very high for this kind of ballistic re-entry vehicle, a location further backward on the capsule surface with lower temperatures was preferred. Predictions showed that at an angle of roughly 85° relative to the flight direction temperatures at around 1500°C could be expected, which is the target range for the application. In Fig. 5 the final position of the experiment is illustrated and Fig. 6 shows the experiment integrated into the spacecraft ablative heat shield.

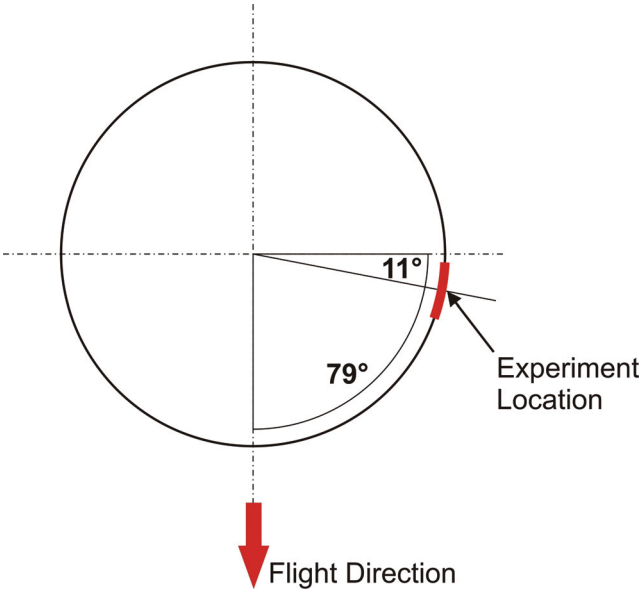

Figure 5: Experiment location on the spacecraft.

4. MISSION OVERVIEW

The Foton missions are Russian unmanned flights with recoverable capsules, which are used to carry out scientific experiments in low Earth orbit under microgravity conditions. They have been flying since 1985 with the type of capsule being in service since the early 1970s. The design is still based on the Vostok spacecraft, which carried Gagarin as the first man into space in 1961.

The Foton-M2 spacecraft was put into orbit by a Soyuz-U launcher on 31 May 2005. The spacecraft remained in orbit for a total of 16 days, thereafter it´s re-entry module returning to earth with the aid of a parachute system.

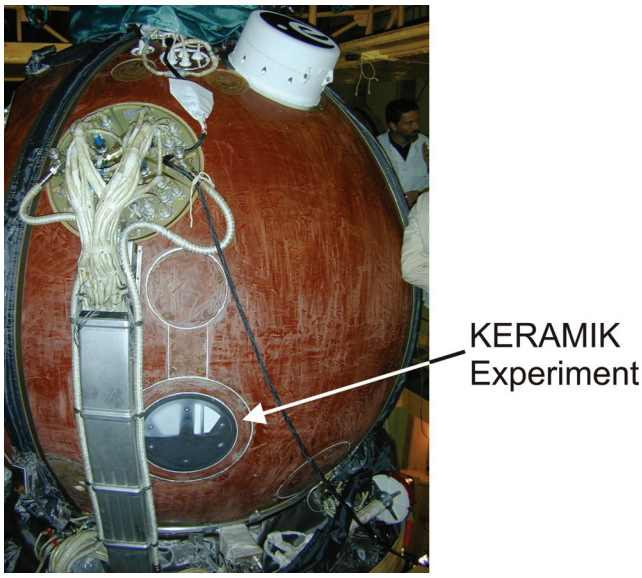

Figure 6: The KERAMIK-Experiment embedded in the heat shield of the FOTON spacecraft.

The experiments on FOTON-M2 covered a wide range of scientific disciplines, including fluid physics, biology, crystal growth, meteoritics, radiation dosimetry and exobiology. Applied research played a role with heat transfer experiments, chemical diffusion experiments and material science investigations. The FOTON-M2 mission provided the reflight opportunity for almost the entire experiment programme originally assigned to FOTON-M1. This was lost due to launcher failure on 15 October 2002.

Table 1: Mission reference data for FOTON-M2

Launcher	Soyuz-U
Spacecraft	Foton-M2
Launch Site	Baikonur Cosmodrome, Kazakhstan
Landing Site	Near town of Kostanay, Kazakhstan
Launch Date	31 May 2005, 14:00 Central European Time
Lift off latitude	63° E
Lift off longitude	45° N
Inclination	63°
Time in orbit	~15 days 20 hour
Orbital period	89.9 minutes
Altitude	262-304km
Return Duration	~30 minutes
Landing	16 June 2005, 10:32 Central European Time

5. LANDING SITE OBSERVATIONS

At the landing site, a visual inspection of the experiment was carried out shortly after touchdown of the capsule. Touchdown took place on agricultural ground which was relatively soft due to intermittent showers the days before landing. Conditions were fair with light clouds and moderate wind.

The capsule impacted the ground quite close to the experiment location. Due to the wind drift it had rolled for about 1m after the initial impact but luckily not over the experiment visible in Fig. 8. The first visual inspection saw the experiment in a very good overall condition with no unexpected issues. All components were firmly in place and deposits of a white to light-gray colour were visible on large areas of the experiment, see Fig. 7.

The ablative thermal protection around the experiment was of a black, charred color with a clearly visible gradient in the degree of charring and ablation with much more severe charring in the areas upstream of the experiment, and less charring on the downstream side. An upward step at the upstream edge of the interface ring had formed due to the ablator recession in that area. At the interface ring in this area, surface erosion was visible as a sign of increased temperatures due to the step formation.

Figure 7: The KERAMIK experiment after flight.

The experiment stayed in place during the transport to the TsSKB-facility in Samara and was disassembled from the capsule about one week later.

Figure 8: The FOTON-M2 spacecraft after touchdown with the KERAMIK experiment near the center of the craft.

6. FLIGHT DATA

6.1 Sensor Locations

The flight data was recorded on board by a small data logger unit with a capacity of 12 channels. Recording frequency was 0.5 Hz. There were nine thermocouples installed, of which four were of type B and five were of type K. In addition one uni-axial accelerometer was installed, mainly for the purpose of time scale correlation. The data logger was configured to record data any time it was switched on and to append each data set after the other until the memory capacity was reached. Some data was recorded during the pre-launch operations during the testing, then the bulk of the data was recorded during the re-entry and the hours following the landing.

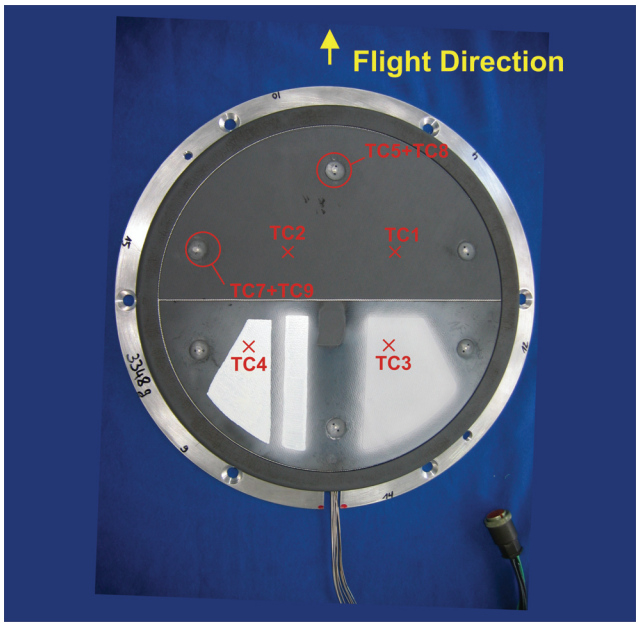

Figure 9: Positions of the surface panel thermocouples TC1 – TC4 and the thermocouples at the attachments.

The type B thermocouples were located on the internal side of the two surface panels. They were positioned in a pattern with two of them beneath the upstream panel and the other two beneath the downstream panel in almost corresponding positions, mirrored over the centerline gap between the panels, illustrated in Fig. 9.

Four of the type K thermocouples were placed in positions at the structural attachment components and one on the aluminum carrier structure. Two of the type K thermocouples were located at the upstream central post. TC5 was placed on the top face of the integral nut in the post, TC8 was located below the foot plate of the post as can be seen in Fig. 10

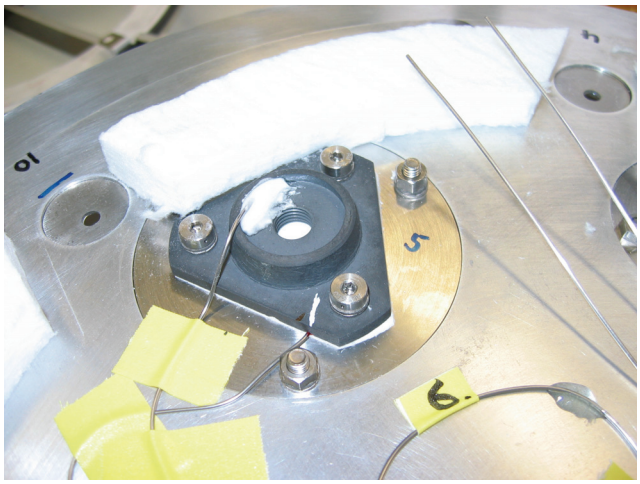

Figure 10: Location of thermocouples TC5 and TC8 at the upstream central post.

It has to be mentioned that between the foot plate of the post and the steel insert on which the post was fixed, a thin layer of ceramic insulation paper was placed for the purpose of a thermal barrier between post and steel insert. The thermocouple was placed between the insulation paper and foot plate.

At the upstream left hand z-post, TC7 was placed in the corner at the upper bend of the z-post, between z-post and nut. TC9 was placed in the lower bend at the z-post, visible in Fig. 11.

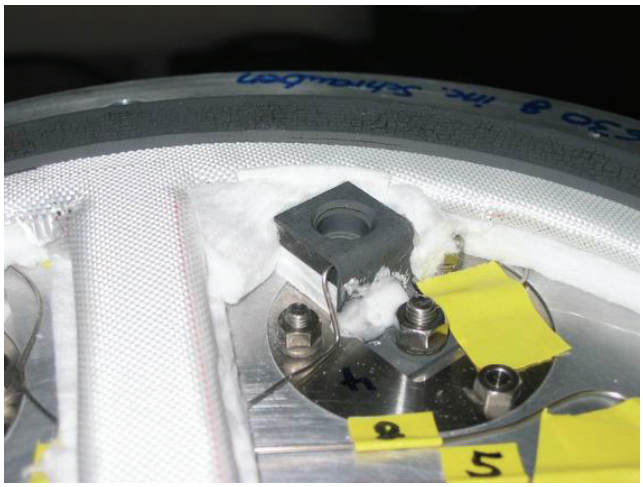

Figure 11: Thermocouples TC7 and TC9 at the z-post.

The fifth type K thermocouple, TC6 was placed in the center of the aluminum carrier structure. The accelerometer was situated in the data handling unit, the measurement direction was aligned with the flight direction during re-entry.

6.2 Acceleration Data

The data handling unit was operated for testing during the pre-launch operations at the launch facility and then, due to restricted memory capacity, remained off-line

for the whole flight until initiation of the re-entry sequence. It was triggered to start operating and recording again when the signal for the firing of the retro engine of the spacecraft was received. This is the zero time point for all the data evaluations hereafter.

The purpose of the accelerometer was to have a redundant correlation option for the measured temperatures with the flight profile in case of any discrepancies with the time scale used in the scpacecraft and in the data recorder. The recorded acceleration data shows indeed that recording began with the retro engine firing and all the major events during re-entry can be identified.

In the beginning of the recording the retro engine firing of 24 seconds is discernible in Fig. 12 which is followed by a period of low deceleration until values increase during the flight in the dense atmosphere. The maximum deceleration value can not be determined since the accelerometer goes into saturation during peak deceleration. After the peak deceleration phase the spikes of the parachute releases can be identified, followed by the glide phase under the parachutes and the landing impact after which the signal stays constant at a medium level due to the tilted position of the capsule. For this experiment the most relevant time frame is the one between 1100 seconds after retro engine ignition when the heat load begins to build up and 1416 seconds when the first drogue parachute is released.

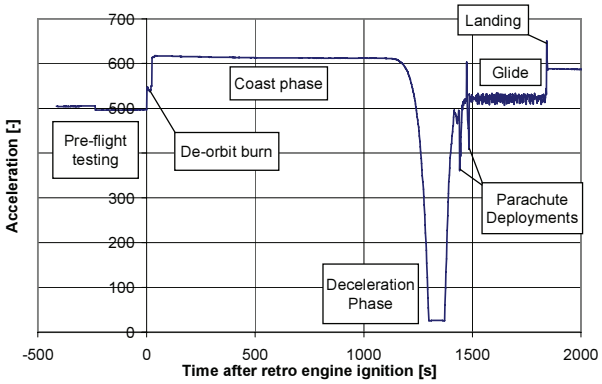

Figure 12: Main acceleration events during re-entry.

6.3 Surface panel temperature data

The recorded temperature data was of very good quality. Due to the information from the accelerometer and from Russian data the temperatures can be correlated accurately to the trajectory of the re-entry flight.

Thermocouples TC1 through TC4 were measuring the surface panel temperatures at their inner face. In Figure 12 the time history of these measurements is presented. The curves show a steep increase of temperatures right from the beginning, followed by an equally steep decrease, typical for the type of ballistic entry profile.

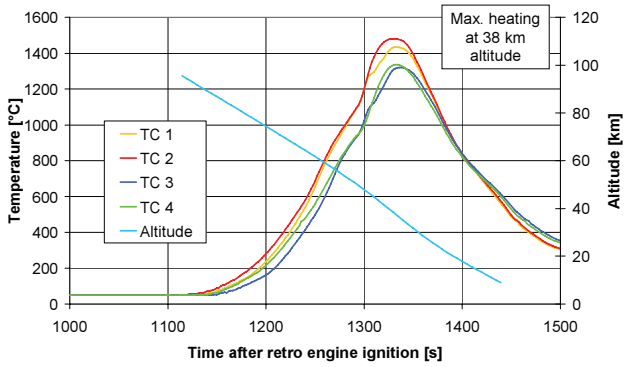

Figure 13: Temperature history of TC1 – TC4.

The maximum temperatures that were recorded by the panel thermocouples are stated in Table 2.

Table 2: Maximum panel temperatures

Thermocouple	Temperature [°C]	Time after retro ignition [s]
TC1	1434	1332
TC2	1481	1330
TC3	1320	1336
TC4	1336	1332

Some interesting features about the temperature recordings at the surface panels can be noticed. In Fig. 13 the graphs of TC1 through TC4 initially follow the same pattern of temperature increase within certain bounds up to roughly 1260 seconds. After that it can be noticed that TC1and TC2 follow almost identical tracks up to 1300 seconds and also TC3 and TC4 are quite close together up to that time. In the the close-up in Fig. 14, after 1300 seconds TC1 and TC3 show a remarkable deviation from the graphs of TC2 and TC4 at practically identical times and in a similar fashion. Since the thermocouples TC1 and TC3 were located at different components, it was concluded that the effect had to be triggered by a change in the heat load.

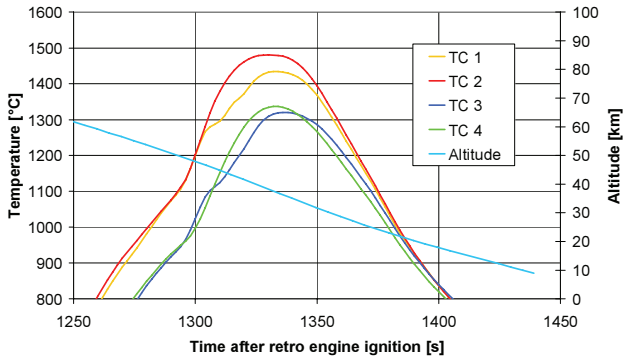

Figure 14: Temperatures of TC1 – TC4 near peak loading.

When the locations of the thermocouple pairs TC1 / TC3 and TC2 / TC4 are looked at in Fig. 9 it becomes obvious that the phenomenon is affecting pairs of thermocouples that are each roughly on one streamline in the flow over the experiment. Therefore a more detailed investigation of the temperature histories of the affected thermocouples was carried out.

When the temperature gradients of the thermocouples TC1 through TC4 are determined, it can be seen in Fig. 15 that there are distinct changes in the gradients which are not uniformly increasing but show a local maximum at roughly 1260 seconds followed by a decrease and then a steep increase at 1290 seconds.

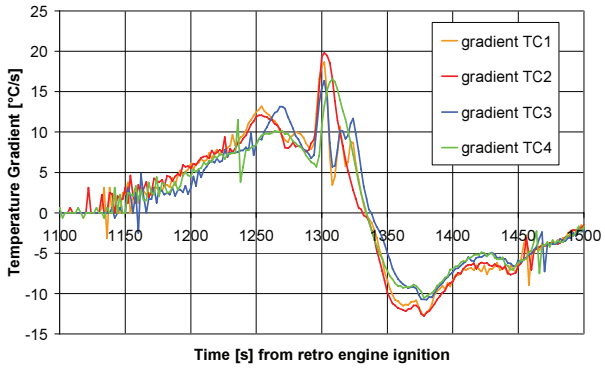

Figure 15: Temperature gradients of TC1 – TC4.

From Fig. 15 it can be concluded that all surface panel thermocouples are affected and that the reason is probably a change in the heat flow into the panels. A reverse analysis was carried out in order to determine the heat flow necessary for producing the recorded temperature data. For this purpose a simple one-dimensional finite-element model was used. The model consisted of 3 layers of material, representative of the panel structure on top, the aluminum carrier structure on the lower side and the high temperature insulation in between. A transient thermal analysis was repeatedly carried out with the heat flux being the input variable and the resulting temperatures the correlation item between analysis and measured data.

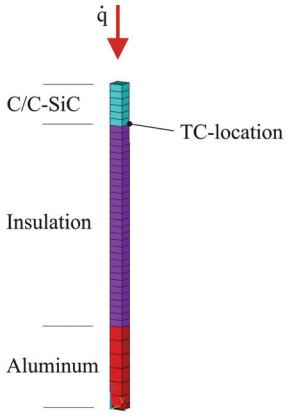

Figure 16: FE-model for heat flux determination.

The analysis covered time intervals of 10 seconds or less if necessary and the heat flux was adjusted until the resulting temperature at the interface between surface panel and insulation met the measured value to within one degree. When this was the case the time span for the analysis was extended for another couple of seconds and the procedure was repeated. That method was applied until the whole re-entry phase from 1100 seconds up to 1400 seconds was covered.

The procedure was applied to the measured data of TC1 and TC2. The results of these analyses are presented in Fig. 17. It can be noticed that the heat fluxes show considerable oscillations, especially the graph of the calculated heat flux for TC1 shows a lot of spikes around the maximum loading.

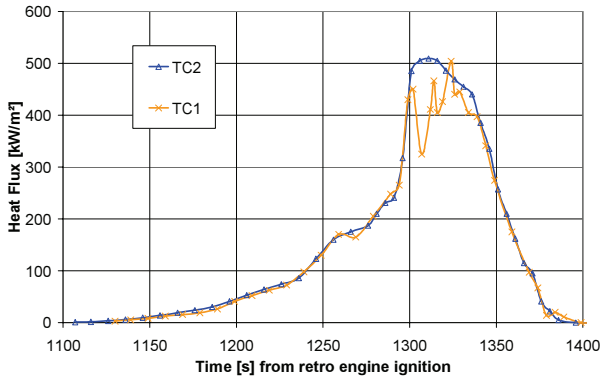

Figure 17: Calculated heat flux for TC1 and TC2.

It can be noted that for both of the calculated heat flux profiles there is a considerable increase in the rate just before 1300 seconds. This is preceded by some smaller oscillations in the increase rate which also can be found in both profiles. These features are still investigated, but it seems very likely they could be produced at least in part by spacecraft oscillating motions, which leads to a changing position of the experiment with regard to the distance to the stagnation point and thus the heat flux values. There remains the question why the temperature profiles and the calculated heat fluxes of TC1 and TC2 show a different behaviour between 1300 and 1340 seconds around maximum heating.

6.4 Attachment components temperature data

The temperatures that were measured in the structural attachments are depicted in Fig. 18. In general the profile is similar to the one for the surface panels from Fig. 13, with the peak values at lower temperatures and slightly moved to later times due to the lag because of the internal placement of the thermocouples. A close view to the data reveals that also the graph of TC7 at the z-post upper corner has an increase in the temperature gradient just before 1300 seconds, like it can be observed for the surface panels.

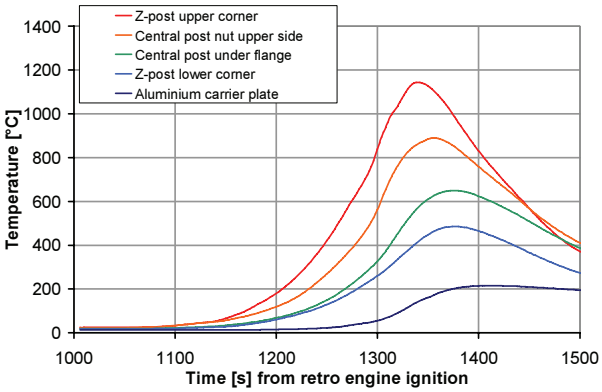

Figure 18: Central post and z-post temperatures.

The temperatures measured at the attachment components show that the approach selected in the design of the attachments and their fastening to the carrier structure was appropriate. The available experiment thickness was very small with only 23.5 mm overall. Therefore it was decided not to fix the C/C-SiC attachment components directly to the aluminum carrier structure but to use an intermediate steel plate, which was inserted into cut-outs in the aluminum plate. In the case of the central post which has a larger conducting cross section there was in addition a thin layer of ceramic insulation paper between C/C-SiC component and steel insert. These measures proved to be working well and even though the temperature of the aluminum carrier plate rose to slightly over 200°C.

In general it can be stated that the entry of FOTON-M2 was a medium-level flight with regard to the possible extreme values of the heat flux and the flight duration. In Fig. 19 the possible extreme trajectories are depicted as they were predicted by TsSKB. The graphs for the steep and the shallow entry trajectory are valid for the stagnation point whereas the graph for the FOTON-M2 mission is the one of the calculated values for the KERAMIK experiment location.

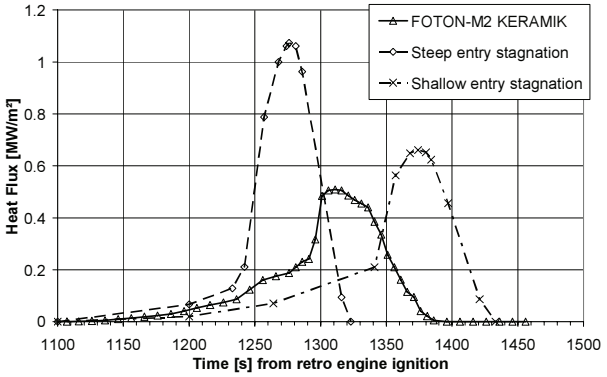

Figure 19: Comparison of the FOTON-M2 trajectory with predicted extremal trajectories.

7. POST FLIGHT COMPONENT CONDITION

7.1 Surface Components

The overall condition of the experiment after flight can be described as very good. The surface panels showed no signs of degradation. Deposits from the ablator reaction products were visible and possibly small deposits from the eroded interface ring.

As a result of the step formation at the upstream boundary of the experiment, a certain area of the interface ring was affected by erosion due to the higher temperatures there. The affected surface area has a maximum depth of approximately 10 mm in flight direction, covering an angle of 53°. The amount of eroded material was very small and there is no measurable decrease in the wall thickness of the interface ring in that location.

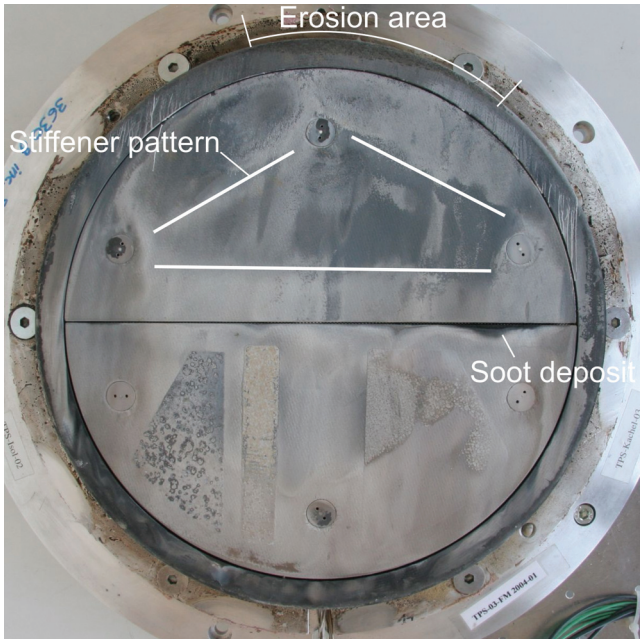

Figure 20: Experiment after flight.

The ablator deposits on the surface panels show an irregular distribution pattern, which is probably influenced by the flow pattern that developed over the experiment, especially with the upward step that was forming with time. In addition, the pattern of the internal stiffeners on the upstream panel is visible from the outside after flight, so it can be concluded that the formation of the deposit layer on this panel was influenced probably by the temperature distribution wihtin the experiment, which was affected by the stiffener locations.

7.2 Internal insulation

After removal of the surface panels the internal condition of the experiment could be examined. Most striking was that the insulation had turned from white to black colour in most areas. This is attributed to the

deposition of soot from ablator reaction products throughout most of the upper layers of the insulation. It is assumed that the soot deposit is the result of a venting process of the experiment with gas saturated with soot entering the experiment internal volume through the sealed gaps between the panels and possibly beneath the interface ring on the upstream border of the experiment. The fact that certain areas appear in white colour is assumed to be the result of an oxidizing process that removes the soot deposit in those areas where temperatures are still high towards the end of the re-entry when the atmospheric pressure is rising quicker and a sufficient amount of oxygen is present to reverse the process of soot deposition.

Figure 21: Post-flight view with removed panels.

7.3 Fasteners

The fasteners that were attaching the surface panels were all firmly in place after flight. During the removal process of the panels the fasteners were tested for their remaining torque. It was discovered that they had lost on average about half of the initial torque that was applied during assembly of the experiment which is a clear indication of the need for improvement of the fastener design with respect to the behaviour under thermal cycling.

7.4 Coatings

The coatings that were applied on the downstream panel were found in a mixed situation. It was obvious that all of them had at least in part experienced major surface alterations. The Yttrium-silicate coating pictured in Fig. 22 showed an area with a distinctive border in which a process with the formation of surface bubbles had taken place. It is not yet clear whether this process includes the coating itself or just the layer of deposit material. The investigation is still going on.

Figure 22: Yttrium-silicate coating after flight.

In the case of the titanium-based coating the picture is slightly different which is noteable from Fig. 23. The coating seems to be affected all over it´s surface with a process resulting in a kind of pockmarks.

The combination layer also in Fig. 23 shows a surface with a gradual change in it´s topology from the upstream to the downstream end. On the upstream half of the coated area the surface shows signs of a liquid phase with a solid skin on top including bubbles. Towards the downstream end these features disappear and the topology is quite similar to the structure of the titanium-based coating with the pockmarked surface.

Figure 23: Titanium-dioxide and Yttrim-titanium coating after flight.

The investigations on the subject of the coatings are still continuing and will be using more detailed methods including sample extraction for microscopic analyses.

8. CONCLUSION

The KERAMIK thermal protection experiment on the FOTON-M2 mission was the first time that a TPS with a rigid surface design manufactured fully in C/C-SiC technology was flown in a re-entry. The flight was very

successful as no major negative issues were detected. It also demonstrated that the design enables high quality measurements of the surface temperatures during flight. These results are a strong case to make the type of TPS the natural choice for advanced research vehicles, when aerodynamic data has to be collected.

Advancements in the technology are possible and will be made. There are certain issues that can be improved, for instance the fastener design. Also the system design can still be advanced towards a lower system weight.

9. ACKNOWLEDGEMENTS

The effort to conduct a thermal protection system experiment on FOTON started in 2001. The flight opportunity was established at a very late time when the M1 mission preparations for launch in October 2002 were already in full swing. So, it was a race against the schedule to complete the experiment in time and make it for spacecraft integration. The author acknowledges the dedication of the manufacturing staff at DLR at that time very much which had resulted in enough spare parts to outfit almost the entire M2 mission. Also the support from the DLR program directorate for the M1 financing is gratefully acknowledged. Unfortunately, the M1 mission failed due to launcher malfunction. Fortunately, all the payloads were taken on to the M2 mission for a re-flight and the effort of ESA, namely Antonio Verga, to include KERAMIK on the M2 list is highly appreciated. Dr. Peter Sickinger and Hans-Günter Bernhardt from Kayser-Threde gave invaluable support in the preparations in Germany and in Russia. Finally, the co-operation with TsSKB in Samara has to be acknowledged very much. Valeri Abrashkin and Sergei Shatochin were dealing with the unusual experiment in unusual ways to make it successful.

10. REFERENCES

[1] Kochendörfer, R., Weihs, H.: „A Fast Processing Route for CMC Materials and Innovative Stand-off Design Concepts“, *First ESA/ESTEC Workshop on Thermal Protection Systems, 5-7 May 1993, ESTEC, Noordwijk, The Netherlands*

[2] Hald, H., Winkelmann, P.: „Post Mission Analysis of the Heat Shield Experiment CETEX for the EXPRESS Capsule“ 48th IAF Congress, October 6-10, 1997, Turin, IAF-97-I.4.01

[3] Hald, H., Petersen, D., Reimer, T., Rühle, F., Winkelmann, P., Weihs, H.: „Development of a CMC-based TPS for two representative Specimens of Cryogenic Tank RLV's“ *AIAA 8th Space Planes and Hypersonic Systems Conference, April 27-30 1998, Norfolk VA, USA*

[4] Weihs, H., Hald, H., Reimer, T., Fischer, I., „Development of a CMC Nose Cap for X-38“, *IAF-01-I.3.01, 52 International Astronautical Congress, Toulouse, 1.-5. October 2001.*